Scalar self-energy for a charged particle in global monopole spacetime with a spherical boundary

E. R. Bezerra de Mello[1*] and A. A. Saharian[1,2†]

[1]*Departamento de Física-CCEN, Universidade Federal da Para íba*
58.059-970, Caixa Postal 5.008, João Pessoa, PB, Brazil

[2]*Department of Physics, Yerevan State University,*
1 Alex Manoogian Street, 0025 Yerevan, Armenia

May 11, 2012

Abstract

We analyze combined effects of the geometry produced by global monopole and a concentric spherical boundary on the self-energy of a point-like scalar charged test particle at rest. We assume that the boundary is outside the monopole's core with a general spherically symmetric inner structure. An important quantity to this analysis is the three-dimensional Green function associated with this system. For both Dirichlet and Neumann boundary conditions obeyed by the scalar field on the sphere, the Green function presents a structure that contains contributions due to the background geometry of the spacetime and the boundary. Consequently the corresponding induced scalar self-energy present also similar structure. For points near the sphere the boundary-induced part dominates and the self-force is repulsive/attractive with respect to the boundary for Dirichlet/Neumann boundary condition. In the region outside the sphere at large distances from it, the boundary-free part in the self-energy dominates and the corresponding self-force can be either attractive or repulsive with dependence of the curvature coupling parameter for scalar field. In particular, for the minimal coupling we show the presence of a stable equilibrium point for Dirichlet boundary condition. In the region inside the sphere the nature of the self-force depends on the specific model for the monopole's core. As illustrations of the general procedure adopted we shall consider two distinct models, namely flower-pot and the ballpoint-pen ones.

1 Introduction

It is well known that different types of topological objects may have been formed in the early Universe by vacuum phase transitions after Planck time [1, 2]. These include domain walls, cosmic strings and monopoles. Global monopoles are heavy and spherically symmetric topological defects. The simplest theoretical model where global monopoles can be obtained is given by a Lagrange density composed by self-coupling iso-triplet scalar field which presents spontaneous

---

[*]E-mail: emello@fisica.ufpb.br

[†]E-mail: saharian@ysu.am

breakdown of global $O(3)$ gauge symmetry [3]. For points far away from the monopole's center, the geometry of the spacetime can be given by the line element below,

$$ds^2 = -dt^2 + dr^2 + \alpha^2 r^2 (d\theta^2 + \sin^2\theta d\varphi^2) \ , \tag{1.1}$$

where the parameter α, smaller than unity, depends on the energy scale where the monopole is formed. The spacetime described by (1.1) has a non-vanishing scalar curvature, $R = 2(\alpha^{-2} - 1)/r^2$, and presents a solid angle deficit $\delta\Omega = 4\pi^2(1 - \alpha^2)$.

Although the geometric properties of the spacetime outside the monopole are very well known, no explicit expressions for the components of the metric tensor in the region inside have been found. Consequently many interesting investigations associated with global monopole consider this object as a point-like defect. In this way calculations of vacuum polarization effects associated with bosonic [5] and fermionic quantum fields [6], in four-dimensional spacetime, present divergence at the monopole's center. Moreover, considering higher-dimensional spacetime, vacuum polarization effects associated with bosonic [7] and fermionic [8] quantum fields, also present similar divergences.

Many years ago, Linet [9] and Smith [10], independently, have shown that an electrically charged particle placed at rest in the spacetime of an idealized cosmic string becomes subjected to a repulsive self-interaction. This self-interaction is a consequence of the distortion of the particle's fields caused by the planar angle deficit associated with the conical geometry. Also it has been shown in [11] that a linear electric or magnetic sources in the spacetime of a cosmic string parallel to the latter, become subject to induced self-interactions. In the spacetime of a global monopole the phenomenon of induced electrostatic self-interaction has been analyzed in [12], considering the defect as a point-like object. In all these analysis, the corresponding self-forces present divergences on the respective defects' core. A possible way to circumvent the divergence problem is to consider these defects as having a non-vanishing radius, and attributing for the region inside a structure. For the cosmic string, two different models have been adopted to describe the geometry inside it. The ballpoint pen model proposed independently by Gott and Hiscock [13], replaces the conical singularity at the string axis by a constant curvature space in the interior region, and the flower-pot model [14], presents the curvature concentrated on a ring with the spacetime inside the string been flat. In [15] the problem of electrostatic self-energy in cosmic string spacetime has been revisited by considering the Gott and Hiscock model for the region inside. Concerning to the global monopole spacetime, the electrostatic self-energy problem has been analyzed considering for the region inside, the flower-pot and ballpoint pen models in [16] and [17, 18], respectively. For both defects it was observed that the corresponding self-forces are finite at their center.[1]

Differently from the electrostatic analysis, the induced self-energy on scalar charged point-like particles on a curved spacetime presents peculiarities due to the non-minimal curvature coupling with the geometry [21, 22]. In the case of of Schwarzschild and Kerr spacetimes, the scalar self-force on a charged particle have been considered in [23] and [24], respectively. Also, the self-energy on scalar particle in the wormhole spacetime has been developed recently in [25]. In the latter, the authors have observed that the self-force vanishes for a conformally coupled massless field. Recently the induced self-energy on a static scalar charged particle in the global monopole has been analyzed in [26] considering a inner structure to it.

In many problems we need to consider a field-theoretical model on the background of manifolds with boundaries on which the dynamical variables satisfy some prescribed boundary conditions. Combined effects of the geometry produced by the global monopole and concentric

---

[1]The analysis of vacuum polarization effect associated with scalar and fermionic fields, considering the flower-pot model for the region inside the monopole, have been developed in [19] and [20], respectively.

spherical boundaries on the polarization of scalar vacuum have been investigated in [27, 28]. Here we decided to continue the analysis of induced self-energies on a static scalar point-like charged particle in the global monopole spacetime, considering at this time the presence of a spherical boundary concentric with the monopole's center, and imposing on the field Dirichlet and Neumann boundary conditions. Following the same line of investigation developed in [26], we consider an inner structure for the monopole; moreover we adopt the core's radius of the monopole, a, being smaller that the boundary's radius, R. In this analysis two distinct situations are taken into account: the charged particle placed at rest outside the boundary followed by the particle inside the boundary. In the latter two different configurations are separately treated, the particle outside the core and inside the core.

Because the analysis is first developed considering a general spherically symmetric structure for the region inside the monopole, two different applications of this formalism are considered, adopting the flower-pot and ballpoint pen models for the region inside. The organization of this paper is the following. In section 2 we present our approach to consider the geometry of the spacetime under consideration, the relevant field equations associated with the scalar charged particle and the boundary conditions obeyed by this field. Also we present the Green functions corresponding to all physical situations. In section 3, explicit formulas for the self-energies ere presented, considering the particle outside the boundary and inside the boundary. As illustrations of the general analysis, in section 4 the flower-pot and ballpoint pen models for the region inside the monopole's core are considered separately. Because the scalar self-energy in the global monopole spacetime has already been investigated, here we are mainly interested in the contribution induced by the boundary. Moreover, we analyze the behavior of the self-energy in various asymptotic regions. In section 5, we present our conclusions and more relevant remarks. We leave for the appendix A specific details related with the obtainment of a simple expression for the energy, and the conditions that the field must obey on the spherical boundary. In the appendix B we provide the procedure adopted to the development of numerical analysis of the self-energy.

2   The system

In this section we present our approach to investigate the induced scalar self-energy, providing a general spherically symmetric model to describe the metric tensor in the region inside the monopole. Also the field equations and boundary conditions obeyed by the field are presented, in order to provide specific expressions for the Green functions considering different situations related with the position of the particle.

2.1   The model

Many investigations of the physical effects associated with a global monopole are developed considering it as an idealized point-like defect. In these analysis the geometry of the whole spacetime is described by line element (1.1). However, a realistic model for a global monopole has to take into account a non-vanishing core radius. Specifically in the system proposed by Barriola and Vilenkin [3], the line element given by (1.1) is attained for the radial coordinate much larger than its characteristic core radius, which depends on the inverse of the energy scale where the global $O(3)$ symmetry is spontaneously broken to $U(1)$. However, explicit expressions for the components of the metric tensor in whole space have not yet been found. Here, in this paper we shall not go into the details about this unsolved problem. Instead, we shall consider a simplified model described by two sets of the metric tensor for two different regions, continuous at a spherical shell of radius a. In the exterior region corresponding to $r > a$, the line element

is given by (1.1), while in the interior region, $r < a$, the geometry is described by the static spherically symmetric line element

$$ds^2 = -dt^2 + v^2(r)dr^2 + w^2(r)(d\theta^2 + \sin^2\theta d\varphi^2) \ . \tag{2.1}$$

As the metric tensor must be continuous at the core's boundary, the functions $v(r)$ and $w(r)$ must satisfy the conditions

$$v(a) = 1 \text{ and } w(a) = \alpha a \ . \tag{2.2}$$

The flower-pot and ballpoint pen models for a global monopole, can be implemented from the general expression given in (2.1) by taking

$$v(r) = 1 \ , \ \ w(r) = r + (\alpha - 1)a \tag{2.3}$$

for the flower-pot model and

$$v(r) = \alpha \left[1 - (r/a)^2(1 - \alpha^2)\right]^{-1/2} \ , \ \ w(r) = \alpha r \ , \tag{2.4}$$

for the ballpoint pen one.

2.2 Scalar self-energy

In this section we analyze a massive scalar field, ϕ, generated by a scalar charge density, ρ, in background of the geometry described by the line element (2.1). In the problem under consideration the particle with the scalar charge is considered as an extra degree of freedom with the fixed location, so its dynamics is not taking into account. In addition, we assume the presence of a spherical boundary, concentric with the global monopole, on which the field obeys Dirichlet or Neumann boundary conditions. We shall discuss the both cases with the charge location outside and inside the spherical boundary. Due to the distortion of the particle's field caused by the geometry of a global monopole and boundary conditions obeyed by the field, a self-action force appears acting on the particle. In this paper we shall consider the influence of a spherical boundary and the monopole's non-trivial core structure on this force by evaluating the corresponding self-energy.

The action associated with a massive scalar field, ϕ, coupled with a scalar charge density, ρ, in a curved background spacetime can be given by

$$S = -\frac{1}{2} \int d^4x \ \sqrt{-g} \ \left(g^{\mu\nu} \nabla_\mu \phi \nabla_\nu \phi + \xi \mathcal{R} \phi^2 + m^2 \phi^2\right) + \int d^4x \ \sqrt{-g} \ \rho \ \phi \ , \tag{2.5}$$

where the first part corresponds to the Klein-Gordon action with an arbitrary curvature coupling, ξ, and the second part takes into account the presence of an interaction term. Note that this type of interaction is used in the Unruh-DeWitt model for a particle detector (see [29]). In the above equation $\mathcal{R}$ represents the scalar curvature and g the determinant of $g_{\mu\nu}$.

The field equation obtained by varying the action with respect to the field reads,

$$\left(\Box - \xi \mathcal{R} - m^2\right) \phi = -\rho \ . \tag{2.6}$$

Because the physical system which we are interested corresponds to a static charged particle, the field is time independent, consequently the equation (2.6) reduces to an effective three-dimensional field equation below:

$$\left(\nabla^2 - \xi \mathcal{R} - m^2\right) \phi = -\rho \ . \tag{2.7}$$

4

Taking the variation of (2.5) with respect to the metric tensor we obtain the energy-momentum tensor associated with this system. For the further discussion it is convenient to write the corresponding expression in the form

$$
\begin{aligned}
T_{\mu\nu} &= \nabla_\mu\phi\nabla_\nu\phi + \frac{1}{2}g_{\mu\nu}\phi\left(\Box - m^2 - \xi\mathcal{R}\right)\phi \\
&\quad + \left[(\xi - 1/4)g_{\mu\nu}\Box + \xi R_{\mu\nu} - \xi\nabla_\mu\nabla_\nu\right]\phi^2 + \rho\,\phi\,g_{\mu\nu}\;,
\end{aligned}
\tag{2.8}
$$

with $R_{\mu\nu}$ being the Ricci tensor.

The energy associated with the scalar particle is given by,

$$
E = -\int d^3x\,\sqrt{-g}\,T_0^0\;.
\tag{2.9}
$$

(Note that the energy considered in [26] is the 0-th covariant component of the four-momentum and differs by sign from (2.9)). In appendix A we show that, considering a spherical boundary with radius R on background of the manifold described by the line element (2.1), this energy may be presented in the form

$$
E = -\frac{1}{2}\int d^3x\,\sqrt{-g}\,\rho\,\phi\;,
\tag{2.10}
$$

for fields obeying, separately, Dirichlet

$$
\phi(r = R, \theta, \varphi) = 0\;,
\tag{2.11}
$$

or Neumann

$$
\partial_r\phi(r, \theta, \varphi)|_{r=R} = 0\;,
\tag{2.12}
$$

conditions on the boundary. In (2.10) the integral is evaluated on the inner, $r \leqslant R$, or outer, $r \geqslant R$, regions, for the case of the particle inside or outside the boundary.

Considering now a point-like scalar charge at rest at the point $\mathbf{x}_p$, the charge density takes the form,

$$
\rho(\mathbf{x}) = \frac{q}{\sqrt{-g}}\delta^3(\mathbf{x} - \mathbf{x}_p)\;.
\tag{2.13}
$$

For this case, the scalar field and the effective three-dimensional Green function defined below,

$$
\left(\nabla^2 - \xi\mathcal{R} - m^2\right)G(\mathbf{x}, \mathbf{x}') = -\frac{\delta^3(\mathbf{x} - \mathbf{x}')}{\sqrt{-g}}\;,
\tag{2.14}
$$

are related by

$$
\phi(\mathbf{x}) = q\,G(\mathbf{x}, \mathbf{x}_p)\;.
\tag{2.15}
$$

So, (2.10) becomes,

$$
E = -\frac{q^2}{2}G(\mathbf{x}_p, \mathbf{x}_p)\;.
\tag{2.16}
$$

The effective three-dimensional Green function that we need for the calculation of the energy diverges at the coincidence limit, providing also a divergent result for the energy. So, we have to apply some renormalization approach to obtain a finite and well defined result. Here we shall use a general renormalization approach in curved spacetime [29], which consists to subtract from the Green function its DeWitt-Schwinger asymptotic expansion. In general there are two types of divergences in the expansion, namely, pole and logarithmic ones. In three-dimensional case which we are interested in, there is only pole divergence. Following [30], the DeWitt-Schwinger expansion for the three-dimensional Green function associated with a massive scalar field reads,

$$
G_{\text{Sing}}(\mathbf{x}, \mathbf{x}') = \frac{1}{4\pi}\left(\frac{1}{\sqrt{2\sigma}} - m\right) + O(\sigma)\;,
\tag{2.17}
$$

where σ is the one-half of the geodesic distance between two points. Adopting the renormalization approach for curved space, the renormalized scalar self-energy is given by

$$E_{\text{Ren}} = -\frac{q^2}{2} \lim_{\mathbf{x} \to \mathbf{x}_p} [G(\mathbf{x}, \mathbf{x}_p) - G_{\text{Sing}}(\mathbf{x}, \mathbf{x}_p)] \,. \tag{2.18}$$

Having the self-energy, we can evaluate the corresponding self-force by using the formula

$$\mathbf{F}_{\text{Ren}} = -\nabla_{\mathbf{x}_p} E_{\text{Ren}} \,. \tag{2.19}$$

An alternative form is obtained by employing the expression of the force $\mathbf{F} = q\nabla_{\mathbf{x}}\phi(\mathbf{x})|_{\mathbf{x}=\mathbf{x}_p}$. For the renormalized self-force this gives

$$\mathbf{F}_{\text{Ren}} = q^2 \lim_{\mathbf{x} \to \mathbf{x}_p} \nabla_{\mathbf{x}} [G(\mathbf{x}, \mathbf{x}_p) - G_{\text{Sing}}(\mathbf{x}, \mathbf{x}_p)]. \tag{2.20}$$

By the Synge's theorem, two expressions (2.19) and (2.20) are equivalent.

2.3 Green function

Taking into account the spherical symmetry of the problem, the scalar Green function can be expressed by the following ansatz,

$$G(\mathbf{x}, \mathbf{x}') = \sum_{l=0}^{\infty} \sum_{m=-l}^{l} g_l(r, r') Y_l^m(\theta, \varphi) Y_l^{m*}(\theta', \varphi') \,, \tag{2.21}$$

with $Y_l^m(\theta, \varphi)$ being the ordinary spherical harmonics. Because here we are analyzing the problem related with scalar charged field in a global monopole spacetime in the presence of a spherical boundary of radius R, we have to solve the differential equation for the Green function, $G(\mathbf{x}, \mathbf{x}')$, by imposing on this function each of the boundary conditions below:

$$G(r, \theta, \varphi; \ r', \theta', \varphi') = 0 \text{ for } r = R \,, \tag{2.22}$$

for Dirichlet boundary condition (DBC), or

$$\partial_r G(r, \theta, \varphi; \ r', \theta', \varphi') = 0 \text{ for } r = R \,, \tag{2.23}$$

for Neumann boundary condition (NBC). In the above expressions, r corresponds to the radial distance of the point closer to the boundary.

In the following calculations we shall adopt a compact notation below,

$$(A + B\partial_r)\, G(\mathbf{x}, \mathbf{x}') = 0 \text{ for } r = R \,, \tag{2.24}$$

and at the end, we specify the values of the parameters associated with each conditions, i.e., $B = 0$ for DBC and $A = 0$ for NBC. Moreover, as it have been mentioned before, we shall assume that the boundary is outside the monopole's core, $R > a$.

In what follows we shall present the steps needed for the calculation of the Green function considering the general expression for the metric tensor (2.1). Substituting (2.21) into (2.14) and using the closure relation for the spherical harmonics, we obtain the radial differential equation below obeyed by the unknown function $g_l(r, r')$:

$$\left[\frac{d}{dr} \left(\frac{w^2}{v} \frac{d}{dr} \right) - l(l+1)v - \xi \mathcal{R} v w^2 - m^2 v w^2 \right] g_l(r, r') = -\delta(r - r') \,, \tag{2.25}$$

6

with the Ricci scalar being given by

$$\mathcal{R} = \frac{2}{w^2} + \frac{4v'w'}{wv^3} - \frac{4w''}{wv^2} - \frac{2(w')^2}{w^2v^2} \ . \tag{2.26}$$

At this point we would like to analyze separately two distinct situations. The first one corresponds to the particle outside the boundary, $r_p = r' > R$, and the second to the particle inside the boundary, $r_p = r' < R$.

2.3.1 Particle outside the boundary

Because we are considering $R > a$, in this first analysis the metric tensor is given by (1.1) and the Ricci scalar reads,

$$\mathcal{R} = 2\frac{1 - \alpha^2}{\alpha^2 r^2} \ , \tag{2.27}$$

consequently (2.25) becomes

$$\left[\frac{d}{dr}\left(r^2 \frac{d}{dr} \right) - \frac{l(l+1) + 2\xi(1 - \alpha^2)}{\alpha^2} - m^2 r^2 \right] g_l(r, r') = -\frac{\delta(r - r')}{\alpha^2} \ . \tag{2.28}$$

The function $g_l(r, r')$ is continuous at $r = r'$, however by integrating (2.28) about this point, the first radial derivative of this function obeys the following junction condition:

$$\partial_r g_l(r, r')|_{r=r'+} - \partial_r g_l(r, r')|_{r=r'-} = -\frac{1}{\alpha^2 r'^2} \ . \tag{2.29}$$

In the region under consideration the two linearly independent solutions of the homogeneous equation corresponding to (2.28) are:

$$\frac{1}{\sqrt{r}} I_{\nu_l}(mr) \ \text{ and } \ \frac{1}{\sqrt{r}} K_{\nu_l}(mr) \ , \tag{2.30}$$

where I_ν and K_ν are the modified Bessel functions of the order

$$\nu_l = \frac{1}{2\alpha} \sqrt{(2l+1)^2 + (1 - \alpha^2)(8\xi - 1)} \ . \tag{2.31}$$

Assuming that for $r > r'$, $g_l(r, r')$, defined below by $g_l^>(r, r')$, goes to zero at infinity, we take for this region

$$g_l^>(r, r') = \frac{a_l}{\sqrt{r}} K_{\nu_l}(mr) \ . \tag{2.32}$$

For the region $R < r < r'$, the radial function, defined as $g_l^<(r, r')$, takes the form:

$$g_l^<(r, r') = \frac{b_l}{\sqrt{r}} K_{\nu_l}(mr) + \frac{c_l}{\sqrt{r}} I_{\nu_l}(mr) \ . \tag{2.33}$$

In the above expression the term with the Macdonald function is a consequence of the presence of the boundary. Following the compact notation specified in (2.24), DBC or NBC imposed on $g_l^<(r, r')$ can be written as:

$$\left(A + B\partial_r \right) g_l^<(r, r') = 0 \text{ at } r = R \ . \tag{2.34}$$

Finally using the junction condition (2.29) together with (2.34), the expression for the radial function g_l reads:

$$g_l(r, r') = \frac{I_{\nu_l}(mr_<)K_{\nu_l}(mr_>)}{\alpha^2 \sqrt{rr'}} - \frac{K_{\nu_l}(mr)K_{\nu_l}(mr')}{\alpha^2 \sqrt{rr'}} \frac{\bar{I}_{\nu_l}(mR)}{\bar{K}_{\nu_l}(mR)} \ , \tag{2.35}$$

where $r_< = \min(r, r')$ and $r_> = \max(r, r')$, and we have used the notations,

$$\bar{F}(z) = ARF(z) + B\tilde{F}(z) , \quad \text{with} \quad \tilde{F}(z) = zF'(z) - \frac{1}{2}F(z) . \tag{2.36}$$

In (2.36), $F'(z)$ denotes the derivative of $F(z)$ with respect to its argument. The second term in the right-hand side of (2.35) goes to zero for $mR \to 0$; also we can verify that g_l or $\partial_{r_<} g_l$ go to zero for $r_< = R$ for DBC and NBC, respectively

2.3.2 Particle inside the boundary

Now in this second analysis we shall consider the particle inside the boundary. In this case two sub cases are present: The particle outside the monopole's core and the particle inside the core. Here it is more appropriate to use for the metric tensor the expression (2.1). Because the functions $v(r)$ and $w(r)$ are continuous at $r = a$, from (2.25) it follows that $g_l(r, r')$ should be continuous at this point. However, due to the second radial derivative of the function $w(r)$ in the expression for the Ricci scalar, a Dirac-delta function contribution appears if the first derivative of this function is not continuous at the monopole's core.[2] Naming by $\check{R} = \bar{R}\delta(r - a)$ the Dirac-delta contribution of the Ricci scalar, the junction condition on the monopole's core is:

$$\partial_r g_l(r, r')|_{r=a^+} - \partial_r g_l(r, r')|_{r=a^-} = \xi\bar{R} \ g_l(a, r') . \tag{2.37}$$

Moreover, the function $g_l(r, r')$ is continuous at $r = r'$, however by integrating (2.25) about this point, the first radial derivative of this function obeys the junction condition below,

$$\partial_r g_l(r, r')|_{r=r'+} - \partial_r g_l(r, r')|_{r=r'-} = -\frac{v(r')}{w^2(r')} . \tag{2.38}$$

Finally we must impose on this function DBC or NBC. These conditions can be implemented as before:

$$(A + B\partial_r) \, g_l(r, r') = 0 \text{ at } r = R . \tag{2.39}$$

Now after this general discussion, let us analyze the solutions of the homogeneous differential equation associated with (2.25) for regions inside the monopole's core. Denoting by $R_{1l}(r)$ and $R_{2l}(r)$ two linearly independent solutions of this equation, we shall assume that $R_{1l}(r)$ is regular at the core center $r = r_c$ and that the solutions are normalized by the Wronskian relation

$$R_{1l}(r)R'_{2l}(r) - R'_{1l}(r)R_{2l}(r) = -\frac{v(r)}{w^2(r)}. \tag{2.40}$$

Moreover, for the region outside the core the solutions are given by (2.30) and (2.31).

Now we can write the function $g_l(r, r')$ as a linear combination of the above solutions with arbitrary coefficients for the regions $(r_c, \min(r', a))$, $(\min(r', a), \max(r', a))$, and $(\max(r', a), R)$. The requirement of the regularity at the core center and the boundary condition, reduce the number of these coefficients to five. These constants are determined by the continuity condition at the monopole's core and at the point $r = r'$, by the junctions conditions given in (2.37) and (2.38), respectively, together with the boundary condition (2.39). In this way we find the

---

[2]For the flower-pot model this fact occurs and has been considered in [16].

8

following expressions:

$$
g_l(r,r') = \frac{R_{1l}(r)K_{\nu_l}(mr')}{\alpha^2\sqrt{ar'}}\frac{M_{\nu_l}(ma)}{R_{1l}(a)}\left[1 - \frac{M_{\nu_l}(mr')\bar{K}_{\nu_l}(mR)}{K_{\nu_l}(mr')\bar{M}_{\nu_l}(mR)}\right] \quad \text{for } r \leqslant a , \qquad (2.41)
$$

$$
g_l(r,r') = \frac{I_{\nu_l}(mr_<)K_{\nu_l}(mr_>)}{\alpha^2\sqrt{rr'}} + D_l^{(+)}(a)\frac{K_{\nu_l}(mr)K_{\nu_l}(mr')}{\alpha^2\sqrt{rr'}}
$$
$$
- \frac{M_{\nu_l}(mr)M_{\nu_l}(mr')}{\alpha^2\sqrt{rr'}}\frac{\bar{K}_{\nu_l}(mR)}{\bar{M}_{\nu_l}(mR)} \quad \text{for } r \geqslant a , \qquad (2.42)
$$

in the case of the charged particle outside the core, $r' \geqslant a$, and

$$
g_l(r,r') = R_{1l}(r_<)[R_{2l}(r_>) + D_l^{(-)}(a)R_{1l}(r_>)] \quad \text{for } r \leqslant a , \qquad (2.43)
$$

$$
g_l(r,r') = \frac{R_{1l}(r')}{\alpha^2\sqrt{ar}}\frac{1}{h_l^{(1)}(a)}\left[K_{\nu_l}(mr)\bar{I}_{\nu_l}(mR) - I_{\nu_l}(mr)\bar{K}_{\nu_l}(mR)\right] \quad \text{for } r \geqslant a , \qquad (2.44)
$$

for the charged particle inside the core, $r' \leqslant a$. In these formulas, $r_< = \min(r,r')$ and $r_> = \max(r,r')$, and we have used the notations:

$$
M_\nu(z) = I_\nu(z) + D_l^{(+)}(a)K_\nu(z) , \qquad (2.45)
$$

$$
D_l^{(+)}(a) = -\frac{a\mathcal{R}_l^{(1)}(a)I_{\nu_l}(ma) - R_{1l}(a)\tilde{I}_{\nu_l}(ma)}{a\mathcal{R}_l^{(1)}(a)K_{\nu_l}(ma) - R_{1l}(a)\tilde{K}_{\nu_l}(ma)} \qquad (2.46)
$$

and

$$
D_l^{(-)}(a) = -\frac{h_l^{(2)}(a)}{h_l^{(1)}(a)} , \qquad (2.47)
$$

with

$$
h_l^{(j)}(a) = \left[aK_{\nu_l}(ma)\mathcal{R}_l^{(j)}(a) - \tilde{K}_{\nu_l}(ma)R_{jl}(a)\right]\bar{I}_{\nu_l}(mR)
$$
$$
- \left[aI_{\nu_l}(ma)\mathcal{R}_l^{(j)}(a) - \tilde{I}_{\nu_l}(ma)R_{jl}(a)\right]\bar{K}_{\nu_l}(mR) . \qquad (2.48)
$$

Here for any function $F(z)$ the notation for $\tilde{F}(z)$ was defined in (2.36), and for a solution $R_{jl}(r)$, with $j = 1, 2$,

$$
\mathcal{R}_l^{(j)}(r) = R'_{jl}(r) + \xi\bar{R}R_{jl}(r) . \qquad (2.49)
$$

The above expressions for g_l are reduced to the previously obtained ones in [26] for $mR \to \infty$. The functions (2.41) and (2.42) obey DBC or NBC for $r' = R$ and for $r_> = R$, respectively. The same conditions are obeyed by (2.44) for $r = R$.

3 Self-energy

In this section we shall calculate the renormalized scalar self-energy considering two situations: the first when the particle is outside the spherical boundary and the second when the particle is inside the boundary. However, the complete treatment of the second case requires the knowledge of the functions inside the monopole's core, $R_{1l}(r)$ and $R_{2l}(r)$. This will be done in the next section as applications of the general formalism developed here, when specific models for the region inside the monopole will be considered.

3.1 Particle outside the boundary

Before considering a specific model for the inner structure of global monopole, let us investigate the self-energy for the case when the charge is outside the spherical boundary. Substituting (2.35) into (2.21), we see that the Green function is expressed in terms of two contributions:

$$G(\mathbf{x}, \mathbf{x}') = G_{\text{gm}}(\mathbf{x}, \mathbf{x}') + G_b(\mathbf{x}, \mathbf{x}') \ , \tag{3.1}$$

where

$$G_{\text{gm}}(\mathbf{x}, \mathbf{x}') = \frac{1}{4\pi\alpha^2\sqrt{rr'}} \sum_{l=0}^{\infty} (2l+1) I_{\nu_l}(mr_<) K_{\nu_l}(mr_>) P_l(\cos\gamma) \tag{3.2}$$

and

$$G_b(\mathbf{x}, \mathbf{x}') = -\frac{1}{4\pi\alpha^2\sqrt{rr'}} \sum_{l=0}^{\infty} (2l+1) K_{\nu_l}(mr) K_{\nu_l}(mr') \frac{\bar{I}_{\nu_l}(mR)}{\bar{K}_{\nu_l}(mR)} P_l(\cos\gamma) \ . \tag{3.3}$$

The first part corresponds to the Green function for the geometry of a point-like global monopole in the absence of boundary and the second one is induced by the boundary. In the formulas above, γ is the angle between the directions (θ, φ) and (θ', φ') and $P_l(x)$ represents the Legendre polynomials of degree l.

The induced scalar self-energy is obtained by taking the coincidence limit in the renormalized Green function. We shall prove later that for points with $r > R$, the boundary-induced term, (3.3), is finite and the divergence takes place in the point-like monopole part only. So, to provide a finite and well defined result for (2.18) we have to renormalize the Green function $G_{\text{gm}}(\mathbf{x}, \mathbf{x}')$ only. First of all we may take $\gamma = 0$ in the above expressions. The renormalized Green function is expressed by:

$$G_{\text{Ren}}(r_p, r_p) = G_{\text{gm,ren}}(r_p, r_p) + G_b(r_p, r_p) \ , \tag{3.4}$$

where

$$G_{\text{gm,ren}}(r_p, r_p) = \lim_{r \to r_p} [G_{\text{gm}}(r, r_p) - G_{\text{Sing}}(r, r_p)] \ . \tag{3.5}$$

In the region outside the monopole's core the radial one-half of geodesic distance becomes $|r - r'|/2$, consequently

$$G_{\text{Sing}}(r, r') = \frac{1}{4\pi} \left(\frac{1}{|r - r'|} - m \right) \ . \tag{3.6}$$

Now, by using $G_{\text{gm}}(r, r')$ given in (3.2), we have:

$$G_{\text{gm,ren}}(r_p, r_p) = \frac{1}{4\pi r_p} \lim_{r' \to r_p} \left[\frac{1}{\alpha^2} \sum_{l=0}^{\infty} (2l+1) I_{\nu_l}(mr_<) K_{\nu_l}(mr_>) - \frac{1}{1-t} \right] + \frac{m}{4\pi} \ , \tag{3.7}$$

where $t = r_</r_>$. In order to evaluate the limit on the right-hand side of this equation, we note that

$$\lim_{t \to 1} \left(\frac{1}{\alpha} \sum_{l=0}^{\infty} t^{l/\alpha + 1/2\alpha - 1/2} - \frac{1}{1-t} \right) = 0 \ . \tag{3.8}$$

So, as a consequence of this relation and replacing in (3.7) the expression $1/(1-t)$ by the first term in the brackets in (3.8), we find[3]

$$G_{\text{gm,ren}}(r_p, r_p) = \frac{S_{(\alpha)}(mr_p)}{4\pi\alpha r_p} + \frac{m}{4\pi} \ , \tag{3.9}$$

---

[3]The expression for the renormalized Green function has also been obtained in [26].

with

$$S_{(\alpha)}(x) = \sum_{l=0}^{\infty} \left[\frac{2l+1}{\alpha} I_{\nu_l}(x) K_{\nu_l}(x) - 1 \right] . \tag{3.10}$$

Finally the complete expression for the scalar self-energy reads

$$E_{\text{Ren}} = -\frac{q^2}{8\pi\alpha r_p} S_{(\alpha)}(m r_p) - \frac{q^2 m}{8\pi} + \frac{q^2}{8\pi\alpha^2 r_p} \sum_{l=0}^{\infty} (2l+1) K_{\nu_l}^2(m r_p) \frac{\bar{I}_{\nu_l}(mR)}{\bar{K}_{\nu_l}(mR)} . \tag{3.11}$$

The convergence of the boundary-induced part on the scalar self-energy can be investigated by analyzing the general term inside the summation of (3.11) for large values of quantum number l, using the uniform asymptotic expansions for large orders of the modified Bessel functions [32]:

$$
\begin{aligned}
I_\nu(\nu z) &\sim \frac{1}{\sqrt{2\pi\nu}} \frac{e^{\nu\eta(z)}}{(1+z^2)^{1/4}} \sum_{k=0}^{\infty} \frac{u_k(w(z))}{\nu^k} , \\
K_\nu(\nu z) &\sim \sqrt{\frac{\pi}{2\nu}} \frac{e^{-\nu\eta(z)}}{(1+z^2)^{1/4}} \sum_{k=0}^{\infty} (-1)^k \frac{u_k(w(z))}{\nu^k} ,
\end{aligned}
\tag{3.12}
$$

where

$$w(z) = \frac{1}{\sqrt{1+z^2}}, \ \eta(z) = \sqrt{1+z^2} + \ln\left(\frac{z}{1+\sqrt{1+z^2}} \right) . \tag{3.13}$$

The relevant expressions for $u_k(z)$ can be found in [32]. In our expression $z = mr/\nu$. Keeping only the leading terms in $1/\nu_l$ for the above expansions, we find

$$
\begin{aligned}
K_{\nu_l}(mr) &\approx \sqrt{\frac{\pi}{2\nu_l}} \left(\frac{2\nu_l}{emr} \right)^{\nu_l} , \\
I_{\nu_l}(mr) &\approx \frac{1}{\sqrt{2\pi\nu_l}} \left(\frac{emr}{2\nu_l} \right)^{\nu_l} .
\end{aligned}
\tag{3.14}
$$

Taking the above expressions and the fact that $2\alpha\nu_l \approx 2l+1 + \frac{(1-\alpha^2)(8\xi-1)}{2(2l+1)}$, after some intermediate steps we find that for large l the term inside the summation of (3.11) behaves as:

$$\pm \alpha \left(R/r_p \right)^{2l/\alpha} , \tag{3.15}$$

and the series converges for $r_p > R$. The positive (negative) sign in the above result corresponds to DBC (NBC).

At large distances from the boundary, assuming that $mr_p \gg 1$, it can be seen that the boundary-induced part in (3.11) is suppressed by the factor e^{-2mr_p} and the boundary-free part dominates. With respect the dependence of the curvature coupling parameter the corresponding force can be either attractive or repulsive (see the numerical examples below). Near the boundary the renormalized self-energy is dominated by the boundary-induced term and behaves as,

$$E_{\text{Ren}} \approx \pm \frac{q^2}{16\pi\alpha} \frac{R^{(1-\alpha)/\alpha}}{r_p^{1/\alpha} - R^{1/\alpha}} . \tag{3.16}$$

The upper (lower) sign corresponds to DBC (NBC). Note that the leading term does not depend on the mass and on the curvature coupling parameter. From (3.16) we conclude that near the spherical boundary the self-force on a charged particle is repulsive with respect to the boundary for DBC and attractive for NBC.

11

The expression for the self-energy is simplified in the case of a massless field. By using the formulas for the modified Bessel functions for small arguments, from general formula (3.11) one finds

$$E_{\text{Ren}} = -\frac{q^2}{8\pi\alpha r_p}\left[S_{(\alpha)}(0) - \sum_{l=0}^{\infty}\frac{2l+1}{2\alpha\nu_l}F_l\left(\frac{R}{r_p}\right)^{2\nu_l}\right]. \tag{3.17}$$

In this formula

$$S_{(\alpha)}(0) = \sum_{l=0}^{\infty}\left(\frac{2l+1}{2\alpha\nu_l} - 1\right), \tag{3.18}$$

and we have defined

$$F_l = \begin{cases} 1, & \text{for DBC} \\ -(2\nu_l - 1)/(2\nu_l + 1), & \text{for NBC} \end{cases}. \tag{3.19}$$

Note that $S_{(\alpha)}(0) > 0$ for $\xi < 1/8$ and $S_{(\alpha)}(0) < 0$ for $\xi > 1/8$. For the special case $\xi = 1/8$ one has $S_{(\alpha)}(0) = 0$. At large distances from the sphere, $r_p \gg R$, the boundary-induced part is suppressed with respect to the boundary-free part by the factor $(R/r_p)^{2\nu_0}$. In this region the self-force for a massless field is attractive for $\xi < 1/8$ and repulsive for $\xi > 1/8$. In the absence of the global monopole, taking $\alpha = 1$, from (3.17) for the case of DBC we get:

$$E_{\text{Ren}}^{(D)}|_{\alpha=1} = \frac{q^2}{8\pi}\frac{R}{r_p^2 - R^2}. \tag{3.20}$$

The corresponding force is repulsive. The expression of the energy for NBC takes the form

$$E_{\text{Ren}}^{(N)}|_{\alpha=1} = -E_{\text{Ren}}^{(D)}|_{\alpha=1} - \frac{q^2}{8\pi R}\ln(1 - R^2/r_p^2), \tag{3.21}$$

and the force is attractive. Note that at large distances from the sphere the decay of the energy in the case of NBC is stronger: $E_{\text{Ren}}^{(N)}|_{\alpha=1} \propto 1/r_p^4$. Taking the limit $R, r_p \to \infty$ with $r_p - R$ fixed, we obtain from (3.20) and (3.21) the interaction energies for a scalar charge with a flat boundary. The corresponding expressions are easily obtained by using the image method. For DBC the sign of the image charge is opposite and the corresponding force is repulsive (for the interaction of scalar point-charges see [33]). For the NBC the normal derivative of the field is zero on the flat boundary and the image charge has the same sign with the attractive force.

In figure 1 we exhibit the behavior for the self-energy given by (3.11) as a function of mr_p for fields obeying DBC and NBC. Here and in the figures below the capital letters near the curves, D and N, represent the respective boundary conditions. In the left panel we consider $\xi = 0$ and for the right panel $\xi = 1$. In both cases we adopted $\alpha = 0.9$ and $mR = 1$. By these plots we can conclude that the boundary-induced contributions do not depend strongly with the curvature coupling, ξ, and for points near the boundary, i.e., with mr_p near the unity, these contributions dominate the behavior of the self-energy; on the other hand for points far from the boundary, the boundary-free contributions dominate; the latter are negative for $\xi = 0$ and positive for $\xi = 1$. At large distances from the boundary, the self-force is attractive with respect to the boundary in the first case and repulsive in the second case. Finally we also can see that for $\xi = 0$, the self-energy presents a stable equilibrium point when the field obeys DBC.

3.2 Particle inside the boundary

The second analysis is for the case when the particle is inside the spherical boundary. Two distinct situations take place: For the particle outside the monopole's core, $r' \geqslant a$, and for the particle inside the core, $r' \leqslant a$. These two situations will be considered separately in the following.
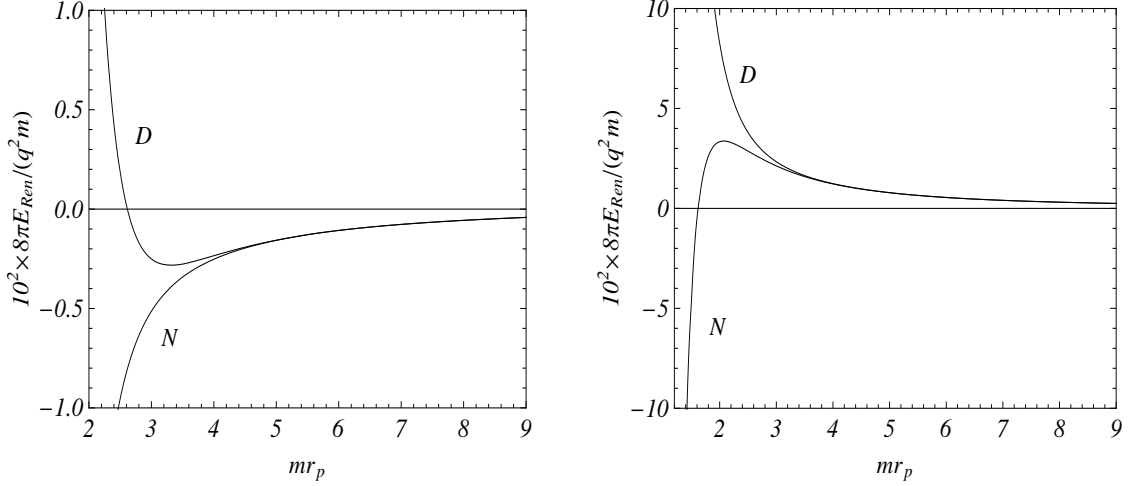
Figure 1: These graphs provide the behavior of the self-energy, $10^2 \times 8\pi E_{\mathrm{Ren}}/(q^2 m)$, as a function of mr_p considering $\xi = 0$ in the left panel and $\xi = 1$ in the right panel. For both cases we adopted $\alpha = 0.9$ and $mR = 1$. The capital letters near the curves represent the boundary condition obeyed by the field, named Dirichlet (D) and Neumann (N), ones.

For the particle outside the monopole, the corresponding Green function can be obtained by substituting (2.42) into (2.21). This procedure allows us to write,

$$G(\mathbf{x}, \mathbf{x}') = G_{\mathrm{gm}}(\mathbf{x}, \mathbf{x}') + G_c(\mathbf{x}, \mathbf{x}') + G_b(\mathbf{x}, \mathbf{x}') \, , \tag{3.22}$$

where $G_{\mathrm{gm}}(\mathbf{x}, \mathbf{x}')$ is given by (3.2),

$$G_c(\mathbf{x}, \mathbf{x}') = \frac{1}{4\pi\alpha^2\sqrt{rr'}} \sum_{l=0}^{\infty} (2l+1) D_l^{(+)}(a) K_{\nu_l}(mr') K_{\nu_l}(mr) P_l(\cos\gamma) \tag{3.23}$$

is the contribution induced by the non-trivial structure of the monopole when the boundary is absent and

$$G_b(\mathbf{x}, \mathbf{x}') = -\frac{1}{4\pi\alpha^2\sqrt{rr'}} \sum_{l=0}^{\infty} (2l+1) M_{\nu_l}(mr) M_{\nu_l}(mr') \frac{\bar{K}_{\nu_l}(mR)}{\bar{M}_{\nu_l}(mR)} P_l(\cos\gamma) \tag{3.24}$$

is the contribution induced by the boundary. We can see that (3.23) and (3.24) contain information about the structure of the monopole' core, through the coefficient $D_l^{(+)}(a)$ given by (2.46).

The induced scalar self-energy is obtained by taking the coincidence limit in the renormalized Green function. As it will be shown later, the only divergence that appears in this limit is in the point-like monopole part. So, in order to provide a finite and well defined result for (2.18), we have to renormalize the Green function $G_{\mathrm{gm}}(\mathbf{x}, \mathbf{x}')$. In fact this has already been done in the last subsection and the result is given by (3.9). Finally the complete expression for scalar self-energy reads

$$
\begin{aligned}
E_{\mathrm{Ren}} = & -\frac{q^2}{8\pi\alpha r_p} S_{(\alpha)}(mr_p) - \frac{q^2 m}{8\pi} - \frac{q^2}{8\pi\alpha^2 r_p} \sum_{l=0}^{\infty} (2l+1) D_l^{(+)}(a) K_{\nu_l}^2(mr_p) \\
& + \frac{q^2}{8\pi\alpha^2 r_p} \sum_{l=0}^{\infty} (2l+1) M_{\nu_l}^2(mr_p) \frac{\bar{K}_{\nu_l}(mR)}{\bar{M}_{\nu_l}(mR)} \, .
\end{aligned}
\tag{3.25}
$$

13

In [26], we have shown that the core-induced part in the self-energy above is finite for points away from the core. It remains to analyze the boundary-induced part for point near the boundary itself.

Before to enter in the details about the boundary-induced part considering specific models for the monopole core, let us first investigate this term for the simpler case considering the monopole as a point-like defect. For this case we have to take the limit $a \to 0$ in (3.25). By analyzing the behavior of the modified Bessel functions for small arguments, we can verify that $D_l^{(+)}(a)$, given in (2.46), goes to zero. This implies that $M_\nu(z) \to I_\nu(z)$, consequently the self-energy reads,

$$E_{\text{Ren}} = -\frac{q^2}{8\pi\alpha r_p}S_{(\alpha)}(mr_p) - \frac{q^2 m}{8\pi} + \frac{q^2}{8\pi\alpha^2 r_p}\sum_{l=0}^{\infty}(2l+1)I_{\nu_l}^2(mr_p)\frac{\bar{K}_{\nu_l}(mR)}{\bar{I}_{\nu_l}(mR)} \ . \tag{3.26}$$

For $\xi > 0$ the boundary-induced part in (3.26) vanishes for $r_p = 0$. For a minimally coupled field, $\xi = 0$, the boundary-induced part is finite at $r_p = 0$ with the only non-zero contribution coming from the $l = 0$ term. Consequently, near the global monopole, $mr_p \ll 1$, the boundary-free part dominates and to the leading order one has $E_{\text{Ren}} \approx -q^2 S_{(\alpha)}(0)/(8\pi\alpha r_p)$. In this region the self-force is attractive with respect to the global monopole for $\xi < 1/8$ and repulsive for $\xi > 1/8$.

For a massless field, the general expression (3.26) takes the form

$$E_{\text{Ren}} = -\frac{q^2}{8\pi\alpha r_p}\left[S_{(\alpha)}(0) - \sum_{l=0}^{\infty}\frac{2l+1}{2\alpha\nu_l F_l}\left(\frac{r_p}{R}\right)^{2\nu_l}\right] \ , \tag{3.27}$$

where F_l is given by (3.19). In deriving (3.27) for NBC we have assumed that $\nu_l \neq 1/2$. If for some $l = l_0$ one has $\nu_{l_0} = 1/2$, the expression for the self-energy is given by (3.27) where now the term $l = l_0$ must be excluded from the summation and the corresponding contribution should be added separately. The latter does not depend on r_p and has the form $q^2(2l_0+1)/(8\pi\alpha^2 R)$. In the absence of the global monopole ($\alpha = 1$), from (3.27) the following results are obtained

$$E_{\text{Ren}}^{(D)}|_{\alpha=1} = \frac{q^2}{8\pi}\frac{R}{R^2 - r_p^2},$$

$$E_{\text{Ren}}^{(N)}|_{\alpha=1} = -E_{\text{Ren}}^{(D)}|_{\alpha=1} + \frac{q^2}{8\pi R}\ln(1 - r_p^2/R^2). \tag{3.28}$$

As for the exterior region, the corresponding force is repulsive/attractive with respect to the sphere for DBC/NBC.

We can verify the convergence of the boundary-induced part, by analyzing the term inside the summation for large values of l. Developing a similar procedure as we did in the last section for the core-induced part, we arrive at the following result:

$$\pm\alpha\left(r_p/R\right)^{2l/\alpha} \ , \tag{3.29}$$

with positive (negative) sign for DBC (NBC). The corresponding series converge for $r_p < R$.

Near the boundary the renormalized scalar-energy is dominated by the boundary-induced term and it behaves as,

$$E_{\text{Ren}} \approx \pm\frac{q^2}{16\pi\alpha}\frac{R^{(1-\alpha)/\alpha}}{R^{1/\alpha} - r_p^{1/\alpha}} \ . \tag{3.30}$$

Here also, the positive (negative) sign corresponds to DBC (NBC). In this region the self-force is repulsive with respect to the boundary for DBC and attractive for NBC.

14

In figure 2 we have plotted the self-energy given by (3.26) versus mr_p for fields with DBC and NBC. The left and right panels are for $\xi = 0$ and $\xi = 1$, respectively. In both cases the graphs are plotted for $\alpha = 0.9$ and $mR = 1$. Also here, we can conclude that the boundary-induced contributions do not depend strongly with the curvature coupling, ξ, for points near the boundary; in fact these contributions dominate the behavior of the self-energy in this region. On the other hand for points near the core's center the boundary-free contributions dominate; the latter are negative for $\xi = 0$ and positive for $\xi = 1$. Finally we observe that for $\xi = 1$, the self-energy presents a stable equilibrium point for the field with DBC.
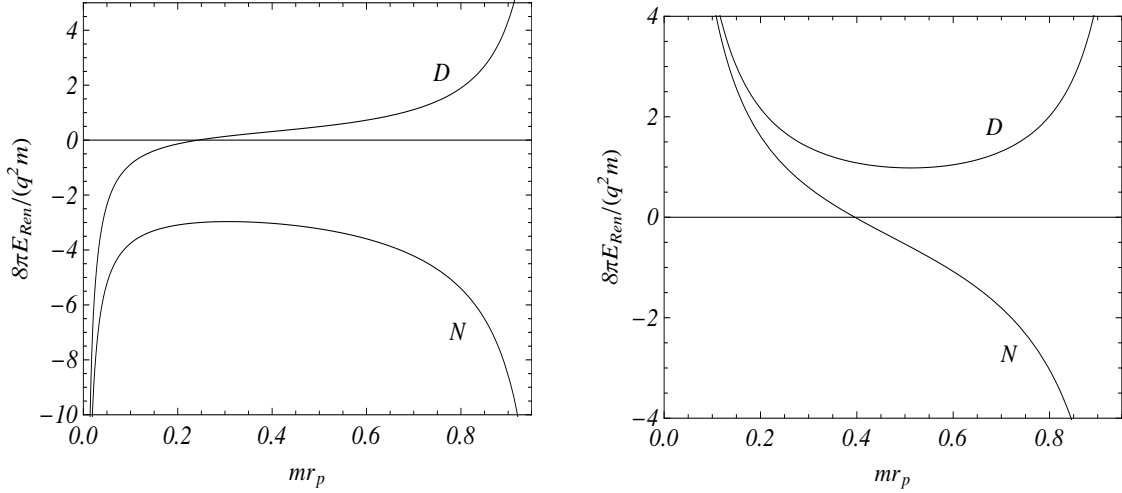

Figure 2: The self-energy inside a spherical boundary as a function of mr_p considering $\xi = 0$ in the left panel and $\xi = 1$ in the right panel. For both cases we adopted $\alpha = 0.9$ and $mR = 1$.

Considering now the general situation, we can see that for the particle inside the core the corresponding Green function can be formally expressed by substituting (2.43) into (2.21):

$$G(\mathbf{x}, \mathbf{x}') = G_0(\mathbf{x}, \mathbf{x}') + G_{\alpha,c}(\mathbf{x}, \mathbf{x}') \ , \tag{3.31}$$

where

$$G_0(\mathbf{x}, \mathbf{x}') = \frac{1}{4\pi} \sum_{l=0}^{\infty} (2l+1) R_{1l}(r_<) R_{2l}(r_>) P_l(\cos\gamma) \ , \tag{3.32}$$

is the Green function for the background geometry described by the line element (2.1) and the term

$$G_{\alpha,b}(\mathbf{x}, \mathbf{x}') = \frac{1}{4\pi} \sum_{l=0}^{\infty} (2l+1) D_l^{(-)}(a) R_{1l}(r) R_{1l}(r') P_l(\cos\gamma) \ , \tag{3.33}$$

is due to the global monopole geometry in the region $r > a$ and the boundary condition obeyed by the field at $r = R$. This information is explicitly contained in the coefficient $D_l^{(-)}(a)$ given by (2.47). We can see that for $mR \to \infty$, this coefficient reduces to

$$D_l^{(-)}(a) = -\frac{a\mathcal{R}_l^{(2)}(a) K_{\nu_l}(ma) - R_{2l}(a)\tilde{K}_{\nu_l}(ma)}{a\mathcal{R}_l^{(1)}(a) K_{\nu_l}(ma) - R_{1l}(a)\tilde{K}_{\nu_l}(ma)} \ . \tag{3.34}$$

For points away from the core's boundary, (3.33) is finite in the coincidence limit.

The renormalized scalar self-energy for a charge inside the core is written in the form

$$E_{\text{Ren}} = -\frac{q^2}{2}G_{0,\text{Ren}}(\mathbf{x}_p, \mathbf{x}_p) - \frac{q^2}{8\pi}\sum_{l=0}^{\infty}(2l+1)D_l^{(-)}(a)R_{1l}^2(r_p) \ , \tag{3.35}$$

where the renormalized Green function is given by

$$G_{0,\text{Ren}}(\mathbf{x}_p, \mathbf{x}_p) = \lim_{\mathbf{x}\to\mathbf{x}_p}\left[G_0(\mathbf{x}, \mathbf{x}_p) - G_{\text{Sing}}(\mathbf{x}, \mathbf{x}_p)\right] \ . \tag{3.36}$$

Because the divergent part of the Green function should have the same structure as (2.17), the above expression provides a finite result.

4   Applications

As we have mentioned in the Introduction, there is no closed expression for the metric tensor in the region inside the global monopole. This situation also happens for the cosmic string spacetime; however two different models have been proposed to describe the geometry inside the string's core, named the ballpoint pen and flower-pot models proposed in [13] and [14], respectively. These two models have been also used in [26] to analyze the self-energy associated with a massive scalar field in the global monopole spacetime. So, motivated by this result, we decided to continue along the same line of investigation considering here both models, and analyzing the influence on the self-energies induced by the spherical boundary.

4.1   Flower-pot model

The first model to be considered is the flower-pot one. For this model the interior line element has the form

$$ds^2 = -dt^2 + dr^2 + [r + (\alpha - 1)a]^2\left(d^2\theta + \sin^2\theta d^2\varphi\right) \ . \tag{4.1}$$

This spacetime corresponds to Minkowski one which can be easily verified by expressing the above line element in terms of the new radial coordinate, $\tilde{r} = r + (\alpha - 1)a$. As we have mentioned before, from the Israel matching conditions for the metric tensors corresponding to (1.1) and (4.1), we find the singular contribution for the Ricci scalar curvature located on the core's surface $r = a$ [19]:

$$\bar{R} = 4\frac{1-\alpha}{\alpha a} \ . \tag{4.2}$$

In the region inside the monopole's core the two linearly independent solutions for the radial functions are:

$$R_{1l}(r) = \frac{I_{l+1/2}(m\tilde{r})}{\sqrt{\tilde{r}}} \text{ and } R_{2l}(r) = \frac{K_{l+1/2}(m\tilde{r})}{\sqrt{\tilde{r}}} \ . \tag{4.3}$$

With these two solutions, we can write explicitly the Green functions in both, interior and exterior regions, and consequently the corresponding self-energies. These expressions depend on the coefficients $D_l^{(+)}(a)$ and $D_l^{(-)}(a)$, which can be explicitly provided.

Considering first the case with the particle outside the core we have,

$$D_l^{(+)}(a) = -\frac{n_l(a)}{d_l(a)} \ , \tag{4.4}$$

16

where

$$n_l(a) = I_{\nu_l}(ma)I_{l+1/2}(m\alpha a)\left[\frac{l+4\xi(1-\alpha)}{\alpha} - \nu_l + \frac{1}{2}\right]$$
$$+ ma\left[I_{\nu_l}(ma)I_{l+3/2}(m\alpha a) - I_{l+1/2}(m\alpha a)I_{\nu_l+1}(ma)\right] , \qquad (4.5)$$

$$d_l(a) = K_{\nu_l}(ma)I_{l+1/2}(m\alpha a)\left[\frac{l+4\xi(1-\alpha)}{\alpha} - \nu_l + \frac{1}{2}\right]$$
$$+ ma\left[K_{\nu_l}(ma)I_{l+3/2}(m\alpha a) + I_{l+1/2}(m\alpha a)K_{\nu_l+1}(ma)\right] . \qquad (4.6)$$

With this coefficient we are in position to write the expression for the complete self-energy (3.25). By this expression we can investigate the behavior of the self-energy due to the core-induced part for points near the core. In fact this analysis has been done in [26], and there we have proved that the boundary-free part

$$E^c = -\frac{q^2}{8\pi\alpha^2 r_p}\sum_{l=0}^{\infty}(2l+1)D_l^{(+)}(a)K_{\nu_l}^2(mr_p) , \qquad (4.7)$$

is divergent near the core. In order to verify this fact, we have analyzed the general term inside the summation for large value of l. By making use of uniform asymptotic expansions (3.12), we get

$$d_l\,(a/r_p)^{2\nu_l} , \qquad (4.8)$$

where

$$d_l = \frac{\alpha - 2\alpha\nu_l + 2l + 8\xi(1-\alpha)}{\alpha + 2\alpha\nu_l + 2l + 8\xi(1-\alpha)}. \qquad (4.9)$$

For large value of l we have $2\alpha\nu_l \approx (2l+1) + \frac{(1-\alpha^2)(8\xi-1)}{2(2l+1)} + \cdots$. Substituting this expansion into (4.8), for the leading term in $1/l$, we obtain

$$\alpha(1-\alpha)\frac{1-8\xi}{4l}\left(\frac{a}{r_p}\right)^{2l/\alpha} . \qquad (4.10)$$

Finally, after some intermediate steps we find:

$$E_{\text{Ren}} \approx q^2\frac{(1-\alpha)(1-8\xi)}{32\pi\alpha a}\ln\left[1 - (a/r_p)^{1/\alpha}\right] . \qquad (4.11)$$

The corresponding self-force is attractive (repulsive) with respect to the core boundary for $\xi < 1/8$ ($\xi > 1/8$).

We may also want to investigate the behavior of the boundary-induced term near the boundary, taking into account this specific model for the core. The boundary-induced term in (3.25) is given by,

$$E^b = \frac{q^2}{8\pi\alpha^2 r_p}\sum_{l=0}^{\infty}(2l+1)M_{\nu_l}^2(mr_p)\frac{\bar{K}_{\nu_l}(mR)}{\bar{M}_{\nu_l}(mR)} . \qquad (4.12)$$

Remembering that $M_\nu(z) = I_\nu(z) + D_l^{(+)}(a)K_\nu(z)$, we can see that for large values of l the coefficient $D_l^{(+)}(a)$ behaves as shown below:

$$D_l^{(+)}(a) \approx \frac{d_l}{\alpha\pi}\left(\frac{ema}{2\nu_l}\right)^{2\nu_l} . \qquad (4.13)$$

17

Adopting also for the modified Bessel functions their asymptotic expansions, we may verify that,

$$M_{\nu_l}(z) \approx \frac{1}{\sqrt{2\pi\nu_l}} \left(\frac{ez}{2\nu_l}\right)^{\nu_l} \left[1 + \frac{d_l}{\alpha}\left(\frac{ma}{z}\right)^{2\nu_l}\right] \approx I_{\nu_l}(z) \tag{4.14}$$

for $z = mR$ or mr_p. So, near the boundary, the dominant contribution on (4.12) is independent of the core, consequently, E^b can be given by (3.30).

In the special case of a massless scalar field, the general expression for the self-energy in the region $a \leqslant r_p \leqslant R$ reduces to

$$E_{\text{Ren}} = -\frac{q^2}{8\pi\alpha r_p}S_{(\alpha)}(0) + \frac{q^2}{8\pi r_p}\sum_{l=0}^{\infty}\frac{2l+1}{2\alpha^2\nu_l}\left\{d_l + \frac{[(r_p/a)^{2\nu_l} - d_l]^2}{F_l(R/a)^{2\nu_l} - d_l}\right\}\left(\frac{a}{r_p}\right)^{2\nu_l}, \tag{4.15}$$

with F_l and d_l defined by the relations (3.19) and (4.9).

Now let us turn our investigation of the self-energy for the region inside the monopole's core. Substituting the functions (4.3) into the formulas (3.32) and (3.33) for the corresponding Green function in the interior region one finds [32],

$$G_0(\mathbf{x}, \mathbf{x}') = \frac{1}{4\pi}\frac{e^{-m\tilde{R}}}{\tilde{R}}, \tag{4.16}$$

with $\tilde{R} = \sqrt{(\tilde{r}')^2 + (\tilde{r})^2 - 2\tilde{r}\tilde{r}'\cos\gamma}$, being γ the angle between the two directions defined by the unit vectors $\hat{\tilde{r}}'$ and $\hat{\tilde{r}}$. Taking $\gamma = 0$ we get $\tilde{R} = |r - r'|$. Because in the flower-pot model the geometry in the region inside the core is Minkowski one, we have $G_0(\mathbf{x}, \mathbf{x}') = G_{\text{Sing}}(\mathbf{x}, \mathbf{x}')$, consequently $G_{0,\text{Ren}}(\mathbf{x}_p, \mathbf{x}_p) = 0$. Consequently, the scalar self-energy in this region is given by

$$E_{\text{Ren}} = -\frac{q^2}{8\pi\tilde{r}_p}\sum_{l=0}^{\infty}(2l+1)D_l^{(-)}(a)I_{l+1/2}^2(m\tilde{r}_p), \tag{4.17}$$

being $\tilde{r}_p = r_p + (\alpha - 1)a$. Due to the fact that the expression derived from (2.47) is too long, we shall not reproduce it in its complete form, only its asymptotic behavior for specific values of l will be provided. Near the core's center, $m\tilde{r}_p \ll 1$,

$$I_{l+1/2}(m\tilde{r}_p) \approx \left(\frac{m\tilde{r}_p}{2}\right)^{l+1/2}\frac{1}{\Gamma(l+3/2)}, \tag{4.18}$$

so the main contribution into the self-energy comes from the lowest mode, $l = 0$, resulting in

$$E_{\text{Ren}} \approx -\frac{q^2 m D_0^{(-)}(a)}{4\pi^2}. \tag{4.19}$$

We can see that for $R \gg a$ the leading term in $D_0^{(-)}(a)$ is boundary independent.

Also we can evaluate the scalar self-energy near the core's boundary. Because $D_l^{(-)}(a)$ presents contributions due to the boundary, to analyze possible divergent contribution of (4.17), we can use asymptotic expansions for large order of the modified Bessel functions. Doing this, after many steps, we find that the numerator, $n_l(a)$, and denominator, $d_l(a)$, of (2.47) are dominated by the terms involving $\bar{I}_{\nu_l}(mR)$. Consequently the leading terms of $D_0^{(-)}(a)$, coincide with the corresponding coefficient when we take $R \to \infty$, providing for the self-energy the same singular behavior as for the boundary-free geometry. The leading term inside the summation in (4.17) behaves as,

$$\frac{(1-\alpha)(1-8\xi)}{4l\alpha a}\left(\frac{\tilde{r}}{\alpha a}\right)^{2l}. \tag{4.20}$$

Finally, taking this expression back into (4.17) we obtain,

$$E_{\text{Ren}} \approx q^2 \frac{(1-\alpha)(1-8\xi)}{32\pi\alpha a} \ln\left[1 - \frac{\tilde{r}_p}{\alpha a}\right] . \tag{4.21}$$

This term does not depend on the mass. As it is seen from (4.21), near the core's boundary the self-force is attractive with respect to this boundary for $\xi < 1/8$ and repulsive for $\xi > 1/8$.

For a massless scalar field, the expression for the self energy inside the core of the monopole is obtained from (4.17) by using the formulas for the modified Bessel functions for small arguments:

$$E_{\text{Ren}} = \frac{q^2}{8\pi\alpha a} \sum_{l=0}^{\infty} \frac{(b_l^{(+)} - l - 1)F_l - (b_l^{(-)} - l - 1)(a/R)^{2\nu_l}}{(b_l^{(+)} + l)F_l - (b_l^{(-)} + l)(a/R)^{2\nu_l}} \left(\frac{\tilde{r}_p}{\alpha a}\right)^{2l} , \tag{4.22}$$

where F_l is defined by (3.19) and

$$b_l^{(\pm)} = 4\xi(1-\alpha) + \alpha/2 \pm \alpha\nu_l. \tag{4.23}$$

From this formula the asymptotic behavior (4.21) is easily obtained for points near the core boundary. The corresponding force linearly vanishes at the core center.

In figure 3 we exhibit, for the flower-pot model, the behavior of the renormalized self-energy for a charged test particle placed inside (left plot) and outside (right plot) the monopole's core as a function of $m\tilde{r}_p$ and mr_p, respectively. In these analysis we consider minimal coupling ($\xi = 0$), $\alpha = 0.9$, $ma = 1/2$ and $mR = 2$. These two plots exhibit the logarithmic singular behavior for the self-energy near the core's boundary; moreover, the left panel shows the influence of the boundary condition obeyed by the field on the external spherical boundary. [4]
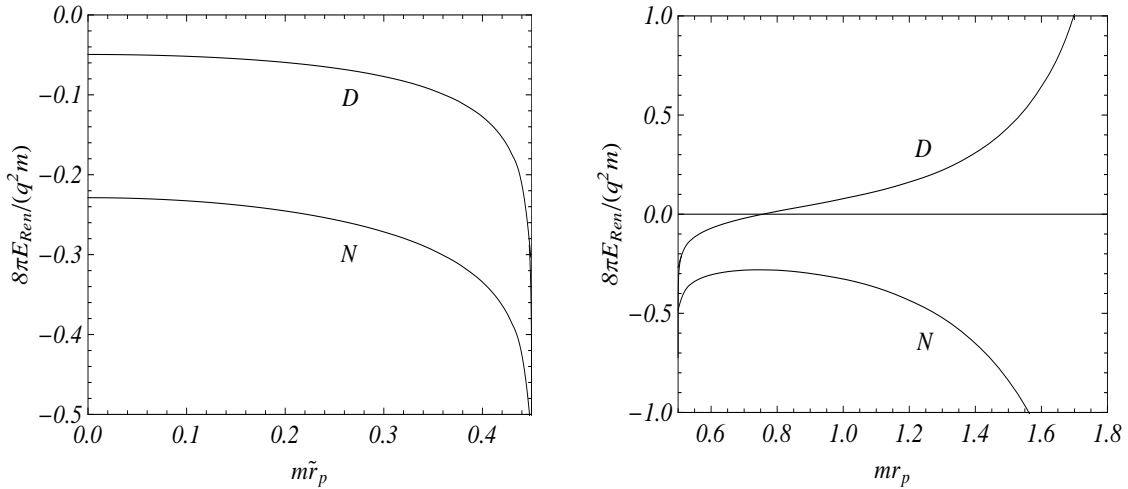
Figure 3: The behavior of the self-energy in the flower-pot model as a function of $m\tilde{r}_p$ and mr_p considering the region inside the core in the left panel and outside the core in the right panel. In both cases we adopted $\alpha = 0.9$, $ma = 1/2$, $mR = 2$ and the graphs are plotted for a minimally coupled field.

---

[4]Another graphs not presented in this paper show that this influence decreases for larger value of mR; specifically for $mR = 4$ no essential difference between the plots has been observed. This is an expected behavior, being a consequence of the dominant contribution on the self-energy due to the core's structure itself.

4.2 Ballpoint pen model

The second model that we shall consider is the ballpoint pen one. For this model, in the region inside the core, we may use the line element below,

$$ds^2 = -dt^2 + v^2(r)dr^2 + \alpha^2 r^2(d\theta^2 + \sin^2\theta d\varphi^2) , \tag{4.24}$$

where the function $v(r)$ is given by the expression (2.4). The only non-vanishing components of the Ricci tensor are:

$$R_r^r = R_\theta^\theta = R_\varphi^\varphi = 2\frac{1-\alpha^2}{\alpha^2 a^2} . \tag{4.25}$$

As to the Ricci scalar, it reads

$$\mathcal{R} = 6\frac{1-\alpha^2}{\alpha^2 a^2} . \tag{4.26}$$

By using the coordinate system corresponding to (4.24), the two independent solutions for the homogeneous radial differential equation associated with (2.25), compatible with the Wronskian normalization (2.40), are

$$R_{1l}(r) = \frac{1}{\sqrt{\alpha r}}P_\chi^{-l-1/2}(z(r)) \text{ and } R_{2l}(r) = \frac{(-1)^l\pi}{2\sqrt{\alpha r}}P_\chi^{l+1/2}(z(r)) , \tag{4.27}$$

being $P_\mu^\nu(x)$ the associated Legendre function and

$$z(r) = \sqrt{1 - (r/a)^2(1-\alpha^2)} , \quad \chi = -\frac{1}{2} + \sqrt{1 - 6\xi - \frac{(ma\alpha)^2}{1-\alpha^2}} . \tag{4.28}$$

Having the radial functions, we are in position to obtain the self-energy for the regions inside and outside the monopole core. Again, these expressions depend on the coefficients $D_l^{(+)}(a)$ and $D_l^{(-)}(a)$.

Considering first the exterior region, the self-energy is given by (3.25). For this case we have,

$$D_l^{(+)}(a) = -\frac{n_l(a)}{d_l(a)} , \tag{4.29}$$

with

$$
\begin{aligned}
n_l(a) &= \sqrt{1/\alpha^2 - 1}I_{\nu_l}(ma)P_\chi^{-l+1/2}(\alpha) \\
&\quad - [(\nu_l + l + 1/2)I_{\nu_l}(ma) + maI_{\nu_l+1}(ma)]P_\chi^{-l-1/2}(\alpha),
\end{aligned} \tag{4.30}
$$

and

$$
\begin{aligned}
d_l(a) &= \sqrt{1/\alpha^2 - 1}K_{\nu_l}(ma)P_\chi^{-l+1/2}(\alpha) \\
&\quad - [(\nu_l + l + 1/2)K_{\nu_l}(ma) - maK_{\nu_l+1}(ma)]P_\chi^{-l-1/2}(\alpha).
\end{aligned} \tag{4.31}
$$

In deriving the expressions (4.30) and (4.31) we have used the relation [31]

$$(1-x^2)\frac{dP_\chi^\mu(x)}{dx} = -\sqrt{1-x^2}P_\chi^{\mu+1}(x) - \mu x P_\chi^\mu(x). \tag{4.32}$$

for the derivative of the associated Legendre function.

In [26] we have shown that, for this model, there is no divergent contribution on the self-energy caused by the core-induced term for points near the core; however, we may wonder about

20

the influence of the core on the boundary-induced term near the boundary. The relevant term to be analyzed is,

$$E^b = \frac{q^2}{8\pi\alpha^2 r_p} \sum_{l=0}^{\infty} (2l+1) M_{\nu_l}^2(mr_p) \frac{\bar{K}_{\nu_l}(mR)}{\bar{M}_{\nu_l}(mR)} \ . \tag{4.33}$$

The procedure to investigate the behavior of this term is similar what we have done in the last subsection. We have to analyze the term inside the summation for large values of l. By using the uniform asymptotic expansions for the modified Bessel functions, we obtain

$$D_l^{(+)}(a) \approx \frac{1}{\pi} \frac{R_{1l}(a)(2\nu_l - 1) - 2a\mathcal{R}_l^{(1)}(a)}{R_{1l}(a)(2\nu_l + 1) + 2a\mathcal{R}_l^{(1)}(a)} \left(\frac{ema}{2\nu_l}\right)^{2\nu_l} \ . \tag{4.34}$$

Considering the solutions (4.27), the term inside the bracket, for large values of l, reads,

$$\frac{R_{1l}(a)(2\nu_l - 1) - 2a\mathcal{R}_l^{(1)}(a)}{R_{1l}(a)(2\nu_l + 1) + 2a\mathcal{R}_l^{(1)}(a)} \approx \frac{(1-\alpha)}{8l^2} [4\chi(1+\chi) - \alpha(1+\alpha)(1-8\xi)] \ . \tag{4.35}$$

So on basis of this result, near the boundary we may approximate $M_{\nu_l}(z) \approx I_{\nu_l}(z)$, for $z = mr_p$ or $z = mR$. Consequently the above expression can be written as,

$$E^b \approx \frac{q^2}{8\pi\alpha^2 r_p} \sum_{l=0}^{\infty} (2l+1) I_{\nu_l}^2(mr_p) \frac{\bar{K}_{\nu_l}(mR)}{\bar{I}_{\nu_l}(mR)} \ , \tag{4.36}$$

which coincides with the boundary-induced term given in (3.26) for the point-like monopole.

The general formula for the self-energy in the region $a \leqslant r_p \leqslant R$ is simplified for a massless scalar field. Taking the limit $m \to 0$ in this formula, one finds

$$E_{\text{Ren}} = -\frac{q^2}{8\pi\alpha r_p} S_{(\alpha)}(0) + \frac{q^2}{8\pi r_p} \sum_{l=0}^{\infty} \frac{2l+1}{2\alpha^2 \nu_l} \left\{ e_l + \frac{[(r_p/a)^{2\nu_l} - e_l]^2}{F_l(R/a)^{2\nu_l} - e_l} \right\} \left(\frac{a}{r_p}\right)^{2\nu_l} \ , \tag{4.37}$$

where we use the notation

$$e_l = \frac{\sqrt{1/\alpha^2 - 1} P_{\chi_0}^{-l+1/2}(\alpha) - (l+1/2+\nu_l) P_{\chi_0}^{-l-1/2}(\alpha)}{\sqrt{1/\alpha^2 - 1} P_{\chi_0}^{-l+1/2}(\alpha) - (l+1/2-\nu_l) P_{\chi_0}^{-l-1/2}(\alpha)}, \tag{4.38}$$

with

$$\chi_0 = -\frac{1}{2} + \sqrt{1 - 6\xi}. \tag{4.39}$$

The core structure is encoded in the function e_l.

Let us now analyze the scalar self-energy for the region inside the core. We need to substitute the functions (4.27) into the formulas (3.32) and (3.33) to construct the corresponding Green function, and in (3.36) to obtain the renormalized self-energy, Eq. (3.35). So we have:

$$G_0(\mathbf{x}, \mathbf{x}') = \frac{1}{8\alpha\sqrt{rr'}} \sum_{l=0}^{\infty} (2l+1)(-1)^l P_\chi^{-l-1/2}(z_<) P_\chi^{l+1/2}(z_>) P_l(\cos\gamma) \ , \tag{4.40}$$

where

$$z_{\gtrless} = \sqrt{1 - (r_{\gtrless}/a)^2(1-\alpha^2)} \ . \tag{4.41}$$

As to DeWitt-Schwinger expansion of the Green function we use (2.17). Taking first the coincidence limit on the angular variables, the radial geodesic distance between two close points inside the monopole can be approximately given by

$$\sqrt{2\sigma} \approx \frac{\alpha|r'-r|}{z(r)} \ . \tag{4.42}$$

So we get

$$G_{\text{Sing}}(r',r) = \frac{z(r)}{4\pi\alpha|r'-r|} - \frac{m}{4\pi} \ . \tag{4.43}$$

Developing some intermediate steps, we obtain the following expression for $G_{0,\text{Ren}}(r',r)$:

$$G_{0,\text{Ren}}(r,r) = \frac{S_\alpha(r/a)}{4\pi\alpha r} + \frac{m}{4\pi} \ , \tag{4.44}$$

where

$$S_\alpha(r/a) = \sum_{l=0}^{\infty} [F(-\chi, \ \chi+1; \ 1/2-l; \ (1-z(r))/2) \, F(-\chi, \ \chi+1; \ 3/2+l; \ (1-z(r))/2) - 1] \tag{4.45}$$

being $F(a,b;c;z)$ the hypergeometric function [31].[5] Consequently the renormalized self-energy becomes,

$$E_{\text{Ren}} = -\frac{q^2 S_\alpha(r_p/a)}{8\pi\alpha r_p} - \frac{q^2 m}{8\pi} - \frac{q^2}{16\alpha r_p} \sum_{l=0}^{\infty} (2l+1)(-1)^l D_l^{(-)}(a)[P_\chi^{-l-1/2}(z(r_p))]^2 \ . \tag{4.46}$$

Let us now analyze the influence of the boundary on the scalar self-energy near the core's center. This can be done by calculating explicitly the coefficient $D_l^{(-)}(a)$. By expressing the associated Legendre function in terms of hypergeometric one by [31],

$$P_\chi^\mu(x) = \frac{1}{\Gamma(1-\mu)} \left(\frac{1+x}{1-x}\right)^{\frac{\mu}{2}} F\left(-\chi, \ \chi+1; \ 1-\mu; \frac{1-x}{2}\right) \ , \tag{4.47}$$

we can see that taking $r \to 0$, we may approximate $z(r) \approx 1 - (r^2/2a^2)(1-\alpha^2)$, and by (4.47) the leading term in the associated Legendre function reads,

$$P_\chi^{-l-1/2}(z(r)) \approx \frac{1}{\Gamma(l+3/2)} \left(\frac{r\sqrt{1-\alpha^2}}{2a}\right)^{l+1/2} \ . \tag{4.48}$$

So the dominant component in the core-induced term is for $l = 0$. Considering also the contribution due to the mass term in (4.46), we have[6]

$$E_{\text{Ren}} \approx -\frac{q^2 D_0^{(-)}(a)\sqrt{1-\alpha^2}}{8\alpha\pi a} - \frac{q^2 m}{8\pi} \ . \tag{4.49}$$

In this case we can also see that for $R \gg a$, the leading term in $D_0^{(-)}(a)$ does not depend on R.

---

[5]The explicit calculation of (4.44) is given in [26].

[6]The contribution due to the background geometry goes to zero for $r_p \to 0$.

For a massless field the general formula for the self-energy inside the core is specified to

$$
\begin{aligned}
E_{\text{Ren}} &= -\frac{q^2 S_\alpha^{(0)}(r_p/a)}{8\pi\alpha r_p} + \frac{q^2}{16\alpha r_p} \sum_{l=0}^{\infty} (-1)^l (2l+1) \\
&\times \frac{F_l f_{l+1/2}^{(-)}(R/a)^{2\nu_l} - f_{l+1/2}^{(+)}}{F_l f_{-l-1/2}^{(-)}(R/a)^{2\nu_l} - f_{-l-1/2}^{(+)}} [P_{\chi_0}^{-l-1/2}(z(r_p))]^2,
\end{aligned}
\tag{4.50}
$$

where the expression for $S_\alpha^{(0)}(r_p/a)$ is obtained from (4.45) by the replacement $\chi \to \chi_0$ and

$$
f_\nu^{(\pm)} = \sqrt{1/\alpha^2 - 1} P_{\chi_0}^{\nu+1}(\alpha) - (\pm\nu_l - \nu) P_{\chi_0}^{\nu}(\alpha). \tag{4.51}
$$

Before to finish this application we want to emphasize that, as in the case of the region outside the core, there is no divergent result on the self-energy given by core-induced part.

In figure 4, for the ballpoint pen model we display the behavior of the renormalized self-energy for a charged test particle placed inside and outside the core as a function of mr_p. Also here we consider the minimal coupling ($\xi = 0$), $\alpha = 0.9$, $ma = 1/2$, and $mR = 2$. For DBC the corresponding self-force is repulsive with respect to the spherical boundary. For NBC the force is repulsive with respect to the boundary for points near the core's center and attractive for points near the boundary.
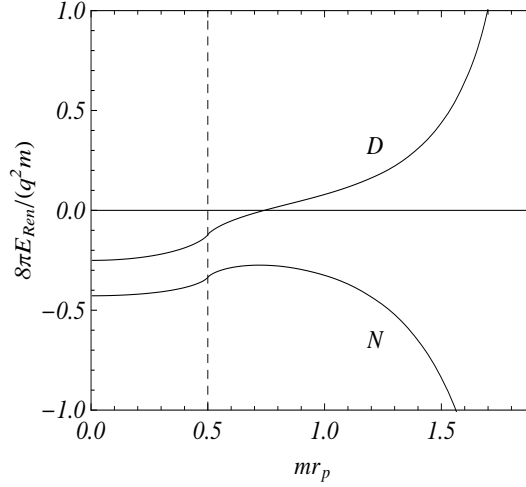

Figure 4: The self-energy in the ballpoint pen model for a minmally coupled scalar field as a function of mr_p, considering $\xi = 0$, $\alpha = 0.9$, $ma = 1/2$ and $mR = 2$.

5 Concluding remarks

In this paper we have analyzed the renormalized self-energy and the self-force associated with a static scalar charged particle placed in the global monopole spacetime, considering a spherical boundary with radius R larger than the core's radius, a. Moreover, on the scalar field associated with the charge, we impose Dirichlet or Neumann boundary conditions on the spherical boundary. The latter modify the self-energy introducing an extra term, named E^b, when compared with the case in the absence of boundary. The main part of this paper concerned on the investigation of the influence of the boundary on this self-energy.

Considering first the particle outside the spherical boundary, we observed that for points near it the self-energy is dominated by the boundary-induced part, which presents a singular behavior given by (3.16). The corresponding self-force is repulsive/attractive with respect to the sphere for DBC/NBC. At large distances from the sphere the self-force can be either attractive or repulsive depending on the curvature coupling parameter. In particular, for a minimally coupled scalar field the force is attractive for both DBC and NBC. For the Dirichlet case, the self-energy has a minimum for some intermediate value of the radial coordinate providing a stable equilibrium point for a point particle.

The second part of the paper is devoted to the analysis of the self-energy in the region inside the spherical boundary. Although at the beginning we have developed a general formalism, only attributing specific models for the region inside the monopole's core, some numerical and closed analysis can be developed. Firstly we have considered a point-like global monopole. In this model for points near the monopole the character of the force depends on the curvature coupling parameter. In the special case of a minimally coupled scalar field the self-force is attractive with respect to the monopole for both DBC and NBC. For a monopole with non-trivial core structure, the force depends on the specific model adopted. We have considered two specific models, namely, the flower-pot and ballpoint pen models. For both these cases we observed that the singular behavior of boundary-induced term in the self-energy is not changed. This behavior is given by (3.30). Besides, in the opposite direction, we also proved that the presence of the boundary does not affect the singular behavior of the core-induced contribution on the self-energy for the flower-pot model. As to the self-energy near the monopole's center, we could see that the presence of the boundary produces a correction on the corresponding quantity when compared with the case of absence of boundary; moreover, this correction becomes weaker for larger values of the sphere radius. In the flower pot model, the force near the core's boundary is attractive (repulsive) with respect to this boundary for $\xi < 1/8$ ($\xi > 1/8$) for both DBC and NBC. In the ballpoint pen model and for a minimally coupled scalar field, the self-force is attractive with respect to the core's center for the region inside the core and also for the exterior points near the core's surface.

The complete analysis for the self-energies, in the regions inside and outside the core, are exhibited numerically in the graphs 3 and 4 for the flower-pot model and ballpoint pen model, respectively. For the flower-pot model, the graphs exhibit the singular behavior near the core's boundary; as to the ballpoint pen one, we were able to provide the behavior of the self-energy for both regions in a single plot.

Acknowledgment

A   Analysis of the self-energy for DBC and NBC

For a static field configuration, by using the field equation (2.6), the $_0^0$-component of the energy-momentum tensor (2.8) is presented in the form

$$T_0^0 = (\xi - 1/4)\nabla^2\phi^2 + \frac{1}{2}\rho\,\phi\;. \tag{A.1}$$

Here we have used the fact that for the geometry under consideration $R_0^0 = 0$. The energy associated with the system under investigation is given by substituting (A.1) into (2.9). It

reads,

$$E = -\int d^3x \; \sqrt{-g} \left[(\xi - 1/4)\nabla^2\phi^2 + \frac{1}{2}\rho \; \phi \right] , \tag{A.2}$$

where the integral is evaluated for the region inside the boundary, $r \leqslant R$, or outside the boundary, $r \geqslant R$, for the cases of the particle inside or outside the boundary, respectively.

Let us analyze the contribution of the integral below, present in (A.2):

$$\int d^3x \; \sqrt{-g} \; \nabla^2\phi^2. \tag{A.3}$$

By applying the Gauss theorem, we can write this integral as,

$$\int d^3x \; \sqrt{-g} \; \nabla^2\phi^2 = \int d^3x \; \sqrt{-g} \; \nabla_i V^i = \int d^3x \; \partial_i(\sqrt{-g} \; V^i) = \oint dS_i \; \sqrt{-g} \; V^i , \tag{A.4}$$

where we have introduced the three-vector $V^i = \nabla^i\phi^2$ and used the fact that for static field $\nabla_\mu V^\mu = \nabla_i V^i$. Moreover, we have admitted that the field goes to zero at infinity. So, the above integral only depends on the the field or its derivative perpendicular to the boundary on the boundary itself. For the spherical boundary we may write $dS_i = dS n_i$, where $n_i = (1,0,0)$ or $n_i = (-1,0,0)$ for the inner or outer regions, respectively. For DBC and NBC, Eqs. (2.11) and (2.12), the surface integral vanishes and, hence, the term with the integral (A.3) does not contribute to the energy. Finally, the energy is presented in the form

$$E = -\frac{1}{2} \int d^3x \; \sqrt{-g} \; \rho\phi . \tag{A.5}$$

Note that in the case of Robin boundary condition on the scalar field the surface term (A.4) does not vanish. However, it should be taken into account that the energy-momentum tensor for a scalar field on manifolds with boundaries in addition to the bulk part contains a contribution located on the boundary. For an arbitrary smooth boundary the expression for the surface energy-momentum tensor is given in [34] (see also [35] for the case of flat boundaries). By using this expression, it can be seen that the part of the field energy coming from the surface energy-momentum tensor exactly cancels the surface term in (A.4) and the energy is given by expression (A.5) for Robin boundary condition as well.

B Procedure adopted in the numerical evaluation

In this appendix we shall provide some technical details related with the numerical analysis approach adopted by us. The most relevant numerical analysis is related with the self-energy associated with the monopole considered as a point-like defect. Because the numerical convergence of this part is very delicate, it is convenient to adopt some trick, as it is exhibited below. We consider the series given by (3.10), where ν_l is given by (2.31). In order to improve the convergence, in the summand we subtract and add the leading term in the asymptotic expansion for large values of l. The latter is easily found by using the uniform asymptotic expansions (3.12):

$$I_\nu(z)K_\nu(z) \approx \frac{1}{2\nu} \left(1 - \frac{z^2}{2\nu^2} \right) + O(\nu^{-4}) . \tag{B.1}$$

So, for the leading term we may write,

$$\frac{2l+1}{\alpha} I_{\nu_l}(mr)K_{\nu_l}(mr) - 1 \approx -\frac{(1-\alpha^2)(8\xi - 1) + 4\alpha^2(mr)^2}{2(2l+1)^2} . \tag{B.2}$$

Finally, we may use in our numerical analysis the expression below:

$$
\sum_{l=0}^{\infty} \left[\frac{2l+1}{\alpha} I_{\nu_l}(mr) K_{\nu_l}(mr) - 1 \right] = \sum_{l=0}^{\infty} \left[\frac{2l+1}{\alpha} I_{\nu_l}(mr) K_{\nu_l}(mr) - 1 \right.
$$
$$
\left. + \frac{(1-\alpha^2)(8\xi-1) + 4\alpha^2(mr)^2}{2(2l+1)^2} \right] - \frac{\pi^2}{16}[(1-\alpha^2)(8\xi-1) + 4\alpha^2(mr)^2] , \qquad \text{(B.3)}
$$

with improved convergence of the series.

References

[1] T. W. Kibble, J. Phys. A. **9**, 1387 (1976).

[2] A. Vilenkin and E. P. S. Shellard, *Cosmic Strings and Other Topological Defects* (Cambridge University Press, Cambridge, England, 1994).

[3] M. Barriola and A. Vilenkin, Phys. Rev. Lett. **63**, 341 (1989).

[4] E. R. Bezerra de Mello, Braz. J. Phys. **31**, 211 (2001).

[5] F. D. Mazzitelli and C. O. Lousto, Phys. Rev. D **43**, 468 (1991).

[6] E. R. Bezerra de Mello, V. B. Bezerra and N. R. Khusnutdinov, Phys. Rev. D **60**, 063506 (1999).

[7] E. R. Bezerra de Mello, J. Math. Phys. **43**, 1018 (2002); E. R. Bezerra de Mello, Phys. Rev. D **73**, 105015 (2006).

[8] E. R. Bezerra de Mello, Phys. Rev. D **76**, 125021 (2007).

[9] B. Linet, Phys. Rev. D **33**, 1833 (1986).

[10] A. G. Smith, in *The Formation and Evolution of Cosmic Strings*, Proceedings of the Cambridge Workshop, Cambridge, England, 1989, edited by G.W. Gibbons, S.W. Hawking, and T. Vachaspati (Cambridge University Press, Cambridge, England, 1990).

[11] E.R. Bezerra de Mello, V.B. Bezerra, C. Furtado and F. Moraes, Phys. Rev. D **51**, 7140 (1995).

[12] E. R. Bezerra de Mello and C. Furtado, Phys. Rev. D **56**, 1345 (1997).

[13] J. R. Gott, Astrophys J. **288**, 422 (1985); W. A. Hiscock, Phys. Rev. D **31**, 3288 (1985).

[14] B. Allen and A. C. Ottewill, Phys. Rev. D **42**, 2669 (1990).

[15] N. R. Khusnutdinov and V.B. Bezerra, Phys. Rev. D **64**, 083506 (2001).

[16] E. R. Bezerra de Mello and A. A. Saharian, Class. Quantum Grav. **24**, 2389 (2007).

[17] D. Barbosa, J. Spinelly and E. R. Bezerra de Mello, Int. J. Mod. Phys D **18**, 1085 (2009).

[18] D. Barbosa, J. Spinelly and E. R. Bezerra de Mello, Int. J. Mod. Phys D **20**, 119 (2011).

[19] E. R. Bezerra de Mello and A. A. Saharian, JHEP **10**, 049 (2006).

[20] E. R. Bezerra de Mello and A. A. Saharian, Phys. Rev. D **75**, 065019 (2007).

[21] L. M. Burko, Class. Quantum Grav. **17**, 227 (2000).

[22] A. G. Wiseman, Phys. Rev. D **61**, 084014 (2000).

[23] A. I. Zelnikov and V. P. Frolov, Zh. Eksp. Teor. Fiz. **82**, 31 (1982) [Sov. Phys. JETP **51**, 191 (1982)].

[24] N. Warburton and L. Barack, Phys. Rev. D **83**, 124038 (2011).

[25] V. B. Bezerra and N. R. Khusnutdinov, Phys. Rev. D **79**, 064012 (2009).

[26] D. Barbosa, U. de Freitas and E. R. Bezerra de Mello, Class. Quantum Grav. **28**, 065009 (2011).

[27] A.A. Saharian and M.R. Setare, Class. Quantum Grav. **20**, 3765 (2003).

[28] A.A. Saharian and M.R. Setare, Int. J. Mod. Phys. A **19**, 4301 (2004).

[29] N. D. Birrell and P. C. W. Davies. *Quantum Fields in Curved Space* (Cambridge University Press. Cambridge. England. 1982).

[30] S. M. Christensen, Phys. Rev. D **17**, 946 (1978).

[31] I. S. Gradshteyn and I. M. Ryzhik, *Table of Integrals, Series and Products* (Academic Press, New York, 1980).

[32] M. Abramowitz and I. A. Stegun, *Handbook of Mathematical Functions* (National Bureau of Standards, Washington DC, 1964).

[33] J. L. Anderson, *Principles of Relativity Physics* (Academic Press, New York, 1967).

[34] A. A. Saharian, Phys. Rev. D **69**, 085005 (2004).

[35] A. Romeo and A. A. Saharian, J. Phys. A **35**, 1297 (2002).